Direct measurement of the mass difference of ^{72}As -^{72}Ge rules out ^{72}As as a promising β-decay candidate to determine the neutrino mass

Z. Ge,[1,*] T. Eronen,[1,†] A. de Roubin,[2] D. A. Nesterenko,[1] M. Hukkanen,[1,2] O. Beliuskina,[1] R. de Groote,[1] S. Geldhof,[1,‡] W. Gins,[1] A. Kankainen,[1] Á. Koszorús,[3] J. Kotila,[4,5] J. Kostensalo,[1,6] I. D. Moore,[1] A. Raggio,[1] S. Rinta-Antila,[1] J. Suhonen,[1] V. Virtanen,[1] A. P. Weaver,[7] A. Zadvornaya,[1] and A. Jokinen[1]

[1]*Department of Physics, University of Jyväskylä, P.O. Box 35, FI-40014 Jyväskylä, Finland*
[2]*Centre d'Etudes Nucléaires de Bordeaux Gradignan, UMR 5797 CNRS/IN2P3 - Université de Bordeaux, 19 Chemin du Solarium, CS 10120, F-33175 Gradignan Cedex, France*
[3]*Department of Physics, University of Liverpool, Liverpool L69 7ZE, United Kingdom*
[4]*Finnish Institute for Educational Research, University of Jyväskylä, P.O. Box 35, FI-40014 Jyväskylä, Finland*
[5]*Center for Theoretical Physics, Sloane Physics Laboratory Yale University, New Haven, Connecticut 06520-8120, USA*
[6]*Natural Resources Institute Finland, Natural Resources, Yliopistokatu 6B, FI-80100 Joensuu, Finland*
[7]*School of Computing, Engineering and Mathematics, University of Brighton, Brighton BN2 4JG, United Kingdom*

(Received 16 March 2021; accepted 25 May 2021; published 15 June 2021; corrected 17 December 2021 and 12 April 2022)

We report the first direct determination of the ground-state to ground-state electron-capture Q value for the ^{72}As to ^{72}Ge decay by measuring their atomic mass difference utilizing the double Penning trap mass spectrometer, JYFLTRAP. The Q value was measured to be 4343.596(75) keV, which is more than a fiftyfold improvement in precision compared to the value in the most recent Atomic Mass Evaluation 2020. Furthermore, the new Q value was found to be 12.4(40) keV (3.1 σ) lower. With the significant reduction of the uncertainty of the ground-state to ground-state Q value combined with the level scheme of ^{72}Ge from γ-ray spectroscopy, we confirm that the five potential ultralow Q-value β^+ decay or electron capture transitions are energetically forbidden, thus precluding all the transitions as possible candidates for the electron neutrino mass determination. However, the discovery of small negative Q values opens up the possibility to use ^{72}As for the study of virtual β-γ transitions.

DOI: 10.1103/PhysRevC.103.065502

I. INTRODUCTION

Neutrino oscillation experiments have given indirect evidence for finite neutrino masses through the observation of neutrino mixing. The fact that neutrinos are massive is the strongest demonstration that the standard model (SM) of electroweak interactions is incomplete and new physics beyond the SM must exist. The oscillation experiments cannot answer the question of the possible Majorana nature of neutrinos and their absolute mass scale [1–3]. Present techniques, which guarantee a model-independent approach for direct measurements of the electron (anti)neutrino mass, are based on a kinematical analysis near the endpoint of β-decay spectra [4–10]. So far, the study of the tritium β-decay end point by means of the electrostatic spectrometer KATRIN (KArlsruhe TRitium Neutrino) has yielded the most stringent upper limit for the electron antineutrino mass, 1.1 eV [90% Confidence Level (C. L.)] [4,5]. The allowed β^--decay transition of $^3\mathrm{H}(1/2^+) \rightarrow {}^3\mathrm{He}(1/2^+)$, with a Q value of 18.59201(7) keV [11], is employed in the KATRIN experiment.

For β decays, the fraction of decay events that fall into an energy interval just below the end-point energy (Q_β) is proportional to Q_β^{-3}; while for electron capture (EC), the event rate proportionality is even steeper. This implies that isotopes with the lowest Q value are desirable [12]. ^{187}Re has been considered for its low Q value of $2.492(30)_{\mathrm{stat}}(15)_{\mathrm{syst}}$ keV [13,14] and because it can be used as a bolometric detector [12,15]. MARE (Microcalorimeter Arrays for a Rhenium Experiment) is the corresponding long-term project carrying the expectations for the future direct neutrino mass measurements [12,15]. Originally based on the development of fast ^{187}Re bolometers, MARE is now also including ^{163}Ho for its low Q value of $2.833(30)_{\mathrm{stat}}(15)_{\mathrm{sys}}$ [16,17], suggested as a unique opportunity for a self-calibrated and high statistics experiment exploiting the enhancement in sensitivity due to the closeness of the ^{163}Ho EC Q value and the ^{163}Dy atomic M lines.

The search for other isotopes that could undergo a low [especially ultralow (<1 keV)] Q-value β decay or EC is of great interest for possible future (anti)neutrino mass determination experiments [18–20]. These transitions include decays into excited states in the daughter nucleus. Whether these types of decays are energetically possible or not can be experimentally determined by measuring the ground-state to ground-state decay Q value and the excitation energy of the state in the daughter nucleus.

*Corresponding author: zhuang.z.ge@jyu.fi
†Corresponding author: tommi.eronen@jyu.fi
‡Present address: KU Leuven, Instituut voor Kern- en Stralingsfysica, B-3001 Leuven, Belgium.

The ultralow Q-value decay branch of ^{115}In $(9/2^+)$ to the first excited state of ^{115}Sn $(9/2^+)$ was first revealed by Cattadori *et al.* [21]. The Q value of this branch was independently measured by Penning trap measurements at Florida State University [22] and at the University of Jyväskylä [23]. With the accurately measured excitation energy of the first excited state of ^{115}Sn from [24], the Q value of this branch was determined to be 0.147(10) keV.

The ground-state to ground-state decay Q value (Q_{gs}) for β^- and EC decays is the difference of atomic masses of the decay parent (M_p) and the decay daughter (M_d):

$$Q_{gs}^{\beta^-/EC} = \left(M_p{}^{\beta^-/EC} - M_d{}^{\beta^-/EC}\right)c^2 \tag{1}$$

and for β^+ decay

$$Q_{gs}^{\beta^+} = Q_{gs}^{EC} - 2m_e c^2, \tag{2}$$

where m_e is the rest mass of the electron and c is the speed of light in vacuum. Combining the Q_{gs} values with the excitation energy of the decay daughter state, $E_i{}^*$ yields the ground-state to excited-state Q value:

$$Q_{E_i{}^*}^{\beta^\pm/EC} = Q_{gs}^{\beta^\pm/EC} - E_i{}^*. \tag{3}$$

For the EC decay, the atomic binding energy B_j, where j denotes the atomic shell of the captured electron, needs to be taken into account. Electron binding energies are typically known to high precision.

The Q values of the decays to excited states in the daughter are normally known with only 1 keV precision or worse [26,28]. The excitation energies E_i^* in the daughter nuclei are typically known with sub-keV precision [27] while the Q_{gs} values are poorly known and commonly lack a value from a direct measurement. Presently, Penning-trap mass spectrometry (PTMS) is the most precise and accurate method for determining atomic masses and Q_{gs} values and routinely reaches sub-keV precision.

Several potential ultralow Q-value β-decay candidates have recently been studied via PTMS, for example ^{89}Sr, ^{131}Cs, ^{135}Cs, and ^{139}Ba [29–31]. Among them, one promising candidate of the first-forbidden unique β^--decay transition, ^{135}Cs $(7/2^+$, ground state$)\rightarrow$ ^{135}Ba $(11/2^-$, second excited state), was confirmed to be an ultralow Q-value decay channel. A Q value of 0.44(31) keV was determined via a measurement at the JYFLTRAP Penning trap [29].

In this work, we report on the Q_{gs}-value determination performed with the JYFLTRAP Penning trap for the promising candidate nucleus ^{72}As [$t_{1/2} = 26.0(1)$ h]. As shown in Fig. 1, the decay daughter ^{72}Ge has four closely lying excited states where the β^+ decay of ^{72}As could proceed with an ultralow Q value. In addition, another state in the decay daughter, which is more than 1 MeV higher in energy from the other four, could possibly be an ultralow Q-value EC decay transition channel. The candidate transitions are listed in Table I. Three out of the five transitions are possibly allowed and the other two are first-forbidden nonunique (FNU) transitions. It is worth noting that the allowed transitions are particularly interesting cases since they have larger branching ratios, enabling the accumulation of more data in a shorter time period and potentially making the case more lucrative for direct (anti)neutrino mass determination [20,28]. In addition, because the decay transition is driven by a single decay matrix element, the β spectral shape is universal, which makes the analysis of the β-decay spectrum simpler.

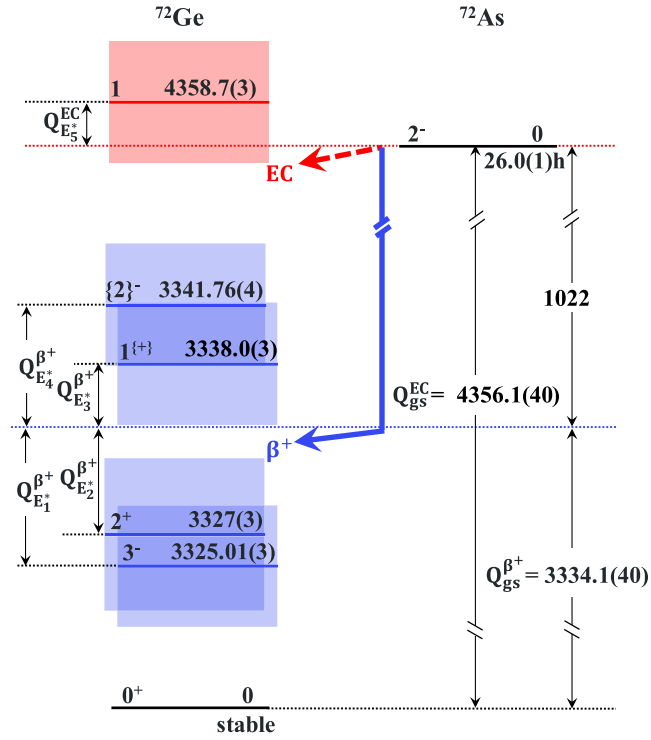

FIG. 1. Partial β^+/EC decay scheme of ^{72}As ground state to excited states in ^{72}Ge. Q_{gs} for both β^+ and EC decays are from AME2020 [25,26] and the energies of the excited states in ^{72}Ge from [27]. The colored shaded bands show the 1σ uncertainty in the Q value, which is almost solely defined by the uncertainty in Q_{gs}. The states below the thick dashed red line marked "EC" and blue line marked "β^+" are energetically possible with electron capture and β^+ decay, respectively. The energies are given in units of keV. See also Table I.

TABLE I. Final states in ^{72}Ge after EC/β^+ decay of ^{72}As 2^- ground state that potentially have a low Q value. The Q_{gs} value is from AME2020 [26] and the excitation energies from [27]. Spin-parity assignments enclosed by braces indicates that these are uncertain, which results in an uncertainty in the decay type, indicated by a {?} in the fourth column. First FNU represents first forbidden nonunique. For the ground-state decay, the Q_{gs}^{EC} value is given. See also Fig. 1 and text for details.

State, i	E^* (keV)	J^π	Decay type	Q (keV)
1	3325.01(3)	3^-	β^+: Allowed	8.9(40)
2	3327(3)	2^+	β^+: 1st FNU	6.9(50)
3	3338.0(3)	$1^{\{+\}}$	β^+: 1st FNU{?}	−4.1(40)
4	3341.76(4)	$\{2\}^-$	β^+: Allowed{?}	−7.9(40)
5	4358.7(3)	1	EC: Allowed{?}	−2.8(40)
gs	0	0^+		4356(4)

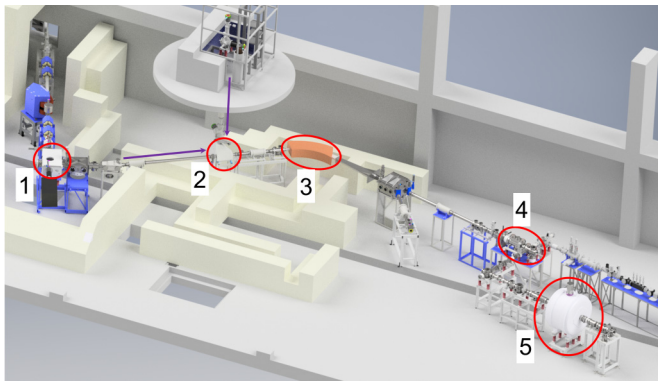

FIG. 2. Schematic overview of the IGISOL facility. The $^{72}As^{+}$ and $^{72}Ge^{+}$ ions were produced with deuteron-induced fusion reactions at the IGISOL target chamber (1). After production and extraction from the gas cell, the ions were guided through an electrostatic bender (2), mass number ($A = 72$) selected with a dipole magnet (3), cooled and bunched in the RFQ cooler-buncher (4) and finally used for the mass-difference measurement in the JYFLTRAP Penning trap setup (5).

The ground-state to ground-state $Q_{gs}^{\beta^+/EC}$ value in AME2020 originates from β^+-decay measurements of $^{72}As(\beta^+)^{72}Ge$, which fully defines the Q value [32,33]. As many previous Penning-trap experiments have already demonstrated large deviations from the Q_{gs} values and masses deduced from β-decay or reaction experiments [34–36], direct mass measurements are strongly desired. With the current precision of the Q_{gs} value, it is difficult to distinguish which of these transitions are energetically possible and further, actually fall into the ultralow Q-value (<1 keV) category. This puzzle is now solved for ^{72}As by a direct mass difference measurement of ^{72}As -^{72}Ge.

II. EXPERIMENTAL DESCRIPTION

The Q_{gs}-value measurement was carried out at the Ion Guide Isotope Separator On-Line facility (IGISOL) using the JYFLTRAP double Penning trap mass spectrometer [37], located at the University of Jyväskylä [38,39]. See Fig. 2 for the layout of the facility. To produce the ions of interest at IGISOL, a thin germanium target with a thickness of about 2 mg/cm^2 was bombarded with a 9-MeV deuteron beam from the K-130 cyclotron. The reaction simultaneously produced both $^{72}As^{+}$ and $^{72}Ge^{+}$ ions.

The produced ions are stopped in the gas cell of the IGISOL light-ion ion guide [40] through collisions with high-purity helium gas at a pressure of about 100 mbar. During this process, the highly charged ions recombine to become predominantly singly charged. The recoils exit the gas cell through a small nozzle into a sextupole ion guide (SPIG) [41]. The ions are guided via the SPIG into high vacuum and get accelerated to 30 keV of energy. A magnetic dipole mass separator with a mass resolving power of about 500 is sufficient to reject all but $A = 72$ ions, where A is the mass number. After the separation, the mass number selected ions are transported through an electrostatic switchyard housing a fast kicker electrode used to chop the beam to have an optimum number of ions. After the switchyard the ions are injected into a radio-frequency quadrupole (RFQ) cooler-buncher [42], which is used to cool and bunch the beam. Finally, the bunches are transported to the downstream JYFLTRAP double Penning trap for the actual frequency ratio measurement.

The JYFLTRAP double Penning trap consists of two cylindrical traps located in a 7 T superconducting magnet. The cooled and bunched ions are confined in a homogeneous magnetic field and a quadrupolar electrostatic potential inside the traps. The first trap, the purification trap, is used as a high-resolution mass separator, while the second trap, precision trap, is utilized for a high-precision mass determination by employment of the conventional time-of-flight ion-cyclotron-resonance (TOF-ICR) method [43,44], or the application of the phase-imaging ion-cyclotron-resonance (PI-ICR) technique [45–47].

The ion beam contained $^{72}Ga^{+}$ as a coproduced impurity. In the first trap an isobarically pure sample of ions was prepared by the mass-selective buffer gas cooling method [48], which provides a typical resolving power $M/\Delta M \approx 10^5$. To prepare a clean sample of $^{72}Ge^{+}$, it was enough to use the mass-selective buffer gas cooling method to remove $^{72}Ga^{+}$, $^{72}As^{+}$ and any other ion species present in the beam. Preparation of a clean sample of $^{72}As^{+}$ required an additional cleaning step. The $^{72}Ge^{+}$ ions were removed with the buffer gas cooling method but to remove $^{72}Ga^{+}$ ions, a higher-resolution Ramsey cleaning method was required [49].

The Q_{gs} value determination is based on the measurement of the cyclotron frequency

$$\nu_c = \frac{1}{2\pi}\frac{q}{m}B \tag{4}$$

for both the decay parent and decay daughter ions. Here q/m is the charge-to-mass ratio of the stored ion and B the magnetic field strength. The Q_{gs} value is obtained through the cyclotron frequency ratio

$$R = \frac{\nu_{c,Ge}}{\nu_{c,As}}, \tag{5}$$

where $\nu_{c,As}$ is the cyclotron frequency for $^{72}As^{+}$ and $\nu_{c,Ge}$ for $^{72}Ge^{+}$. During this experiment, we alternated between $^{72}As^{+}$ and $^{72}Ge^{+}$ cyclotron frequency measurements every few minutes to minimize contribution of the magnetic field fluctuation in the measured cyclotron frequency ratio. Still, a linear interpolation was used to obtain the magnetic field at the moment of the parent cyclotron frequency measurement.

In this work, the PI-ICR technique was used to measure the cyclotron frequencies [45–47]. This technique is about 25 times faster reaching a certain precision compared to the TOF-ICR method. In particular, the measurement scheme number 2 described in Ref. [46] was utilized to directly measure the cyclotron frequency.

Two timing patterns, one called magnetron and the other cyclotron, were used, see Ref. [45]. These patterns are otherwise identical except for the switching on instant of the π pulse that converts the ions' cyclotron motion to magnetron. In the magnetron pattern the ions predominantly revolve in the trap for a time duration t (accumulation time) with mag-

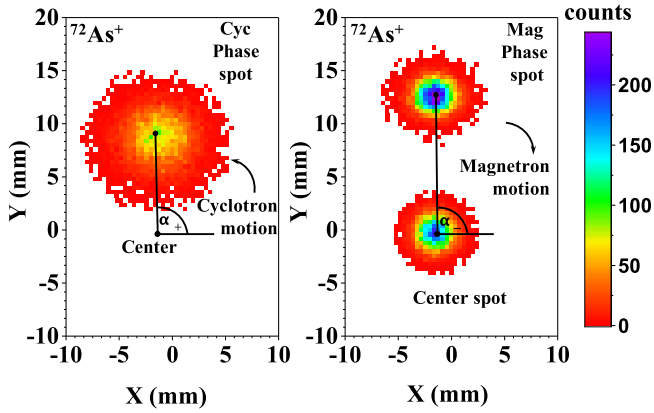

FIG. 3. Center, cyclotron phase, and magnetron phase spots of $^{72}As^+$ on the position-sensitive MCP detector after the PI-ICR excitation pattern with an accumulation time of 321 ms. The figure comprises all data recorded in the experiment. The cyclotron phase spot is displayed on the left side and the magnetron phase spot with a center spot on the right. The angle difference between the two spots relative to the center spot is utilized to deduce the cyclotron frequency of the measured ion species. The color bar illustrates the number of ions in each pixel.

netron motion while in the cyclotron pattern the ions revolve with cyclotron motion. The exact knowledge of the switch-on time difference t is essential. The used patterns produce so-called magnetron and cyclotron spots or phases on the position-sensitive microchannel plate (MCP) detector [50]. Additionally, it is necessary to measure the motional center spot. With these data, it is then possible to obtain the angle between the cyclotron and magnetron motion phases with respect to the center spot

$$\alpha_c = \alpha_+ - \alpha_-, \tag{6}$$

where α_+ and α_- are the polar angles of cyclotron and magnetron phases, respectively. Finally, the cyclotron frequency ν_c is deduced from

$$\nu_c = \frac{\alpha_c + 2\pi n_c}{2\pi t}. \tag{7}$$

n_c is the number of complete revolutions during the phase accumulation time t. The measurement is set up so that α_c will be small in order to minimize systematic shifts due to image distortion by choosing t to be as close to integer multiples of ν_c period as possible. This minimized the angle α_c to ensure minimal influence from the interconversion of magnetron and cyclotron motions [46,51]. In these measurements α_c did not exceed a few degrees.

The accumulation time t for both $^{72}Ge^+$ and $^{72}As^+$ ions during the interleaved measurement was about 321 ms, which ensured that the cyclotron spot was not overlapping with any possible isobaric, isomeric, or molecular contamination.

The collected magnetron and cyclotron phase spots of $^{72}As^+$ ions are plotted in the left and right panels of Fig. 3. The delay of the cyclotron motion excitation was repeatedly scanned over one magnetron period and the final extraction delay was varied over one cyclotron period to account for any residual magnetron and cyclotron motion that could shift the different spots. These constituted in a total of $5 \times 5 = 25$ scan points for both magnetron and cyclotron phase spots. As the decay parent $^{72}Ge^+$ and the decay daughter $^{72}As^+$ ions were produced simultaneously at IGISOL and were alternatively measured in JYFLTRAP after separation and purification of the samples, a direct doublet measurement was realized. The measurement of the ν_c of the ions $^{72}Ge^+$ and $^{72}As^+$ was performed continuously for a total duration of about 6.5 h.

The frequency measurement directly yields the Q_{gs}^{EC} value [see Eq. (8)] via the cyclotron frequency ratio R

$$Q_{gs}^{EC} = (R-1)(M_d - m_e)c^2 + \Delta B_{m,d}, \tag{8}$$

where M_d is the atomic mass of the decay daughter (^{72}Ge). $\Delta B_{m,d}$ is a term that takes into account the electron binding energy difference of the decay parent-daughter atoms ($\approx$2.6 eV) using ionization energies from the National Institute of Standards and Technology (NIST) [52]. Since both the parent and daughter have the same A/q, the mass-dependent error effectively becomes negligible compared to the statistical uncertainty achieved in the measurement [53]. Additionally, due to the fact that the mass difference $\Delta M/M$ of ^{72}Ga and ^{72}As is smaller than 10^{-4}, the contribution to the Q_{gs}^{EC} value from the mass uncertainty (0.08 keV/c^2) of the reference ^{72}Ge is negligible.

III. RESULTS AND DISCUSSION

The data was collected by initiating a ν_c measurement of $^{72}As^+$ for four full scan rounds (one round consisting of 5×5 points for both magnetron and cyclotron phases) followed by measurement of $^{72}Ge^+$ also for four full scan rounds. After, a center spot was recorded with $^{72}Ge^+$ ions. In total, these steps lasted about 7 min in total and were repeated over a period of 6.5 h.

For each repetition, positions of each spot were determined using the maximum likelihood method and the phase angles were calculated to deduce the cyclotron frequencies. Consecutive fitted cyclotron frequencies of $^{72}Ge^+$ were linearly interpolated to the time of the measurement of $^{72}As^+$. This interpolated frequency was used to deduce the cyclotron resonance frequency ratio R. In this manner, a total of about 70 frequency ratios were obtained. Contribution of temporal fluctuations of the magnetic field to the final frequency ratio uncertainty was less than 10^{-10} since the frequency measurements of the ion pair were tightly interleaved.

The incident ion rate was limited to a maximum of 5 detected ions/bunch with the median value being around 2 ions/bunch. Bunches with more than 5 ions were rejected from the analysis in order to reduce a possible cyclotron frequency shift due to ion-ion interactions [53,54]. Count-rate class analysis [54] was used to confirm that the frequency was indeed not shifting.

The frequency shifts due to ion image distortions were well below the statistical uncertainty. This was ensured by keeping α_c of Eq. (6) small (<4 degrees). The weighted mean ratio $\overline{R}$ of the single ratios for PI-ICR data was calculated along with the inner and outer errors. The ratio of inner and outer

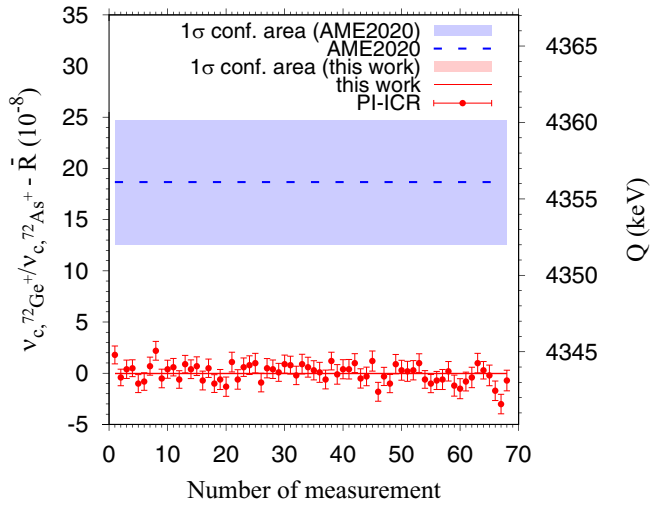

FIG. 4. Comparison of results from this work and AME2020. The left axis shows the corresponding frequency ratio deviation from the measured value and the right axis the Q value. The red points are the data points and the solid horizontal red line with the shaded area the final value. The dashed blue line is the AME2020 value (shaded area is the 1σ uncertainty).

errors, otherwise known as the Birge ratio [55], was found to be 0.987. The larger of the errors, the outer error, was taken as the final uncertainty. In Fig. 4, the results of the analysis are compared to the literature values. The final frequency ratio $\overline{R}$ and the resulting Q_{gs}^{EC} value are 1.0000648351(11) and 4343.596(75) keV, respectively.

To check the reliability of the above interpolation method, a polynomial fitting method [45,56] was also used to deduce the frequency ratio. The temporal evolution of the measured cyclotron frequencies $\nu_{c,p}(t)$ for parent $^{72}As^{+}$ ions and $\nu_{c,d}(t)$ for daughter $^{72}Ge^{+}$ ions can be described with the same polynomial function $f(t)$ and the frequency ratio R:

$$\nu_{c,p}(t) = f(t), \quad \nu_{c,d}(t) = R\nu_{c,p}(t) = Rf(t). \tag{9}$$

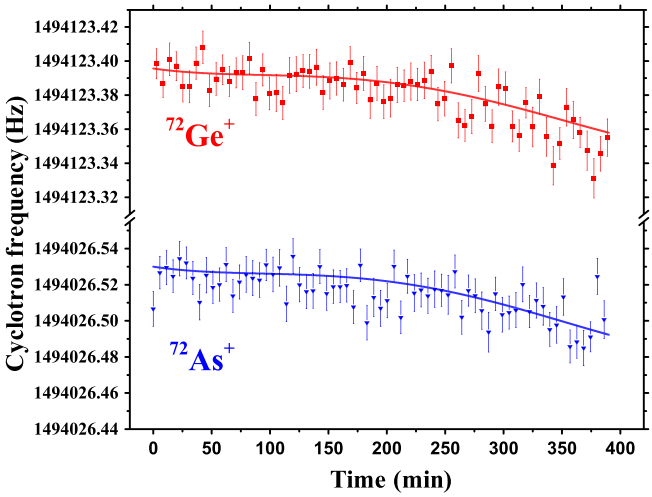

FIG. 5. Cyclotron frequency ratio determination using a simultaneous polynomial fit to the measured cyclotron frequency data. The reduced χ^2 was 0.95. See text for more details.

TABLE II. Final results based on the analysis of the mean cyclotron frequency ratio between the daughter ($^{72}Ge^{+}$) and parent ($^{72}As^{+}$) ions. Q_{gs}^{EC} value and the mass excess (ME) of ^{72}As determined in this work in comparison to the AME2020 values [25].

	Q_{gs}^{EC} (keV)	ME (keV/c^2)
This Work	4343.596(75)	−68242.305(106)
AME2020	4356(4)	−68230(4)

The order of the polynomial was chosen to be four, which gives the smallest reduced χ^2 of the fit. The result is shown in Fig. 5, where individual frequency points are shown with the fit. The frequency ratio obtained from the polynomial fit agrees well with the one obtained from the linear interpolation analysis within a combined 1σ uncertainty.

The final Q_{gs}^{EC} value and the mass excess of ^{72}As obtained from the mean cyclotron frequency ratio is given in Table II. The Q_{EC} value from this work is a factor of 54 more precise and 12.4(40) keV smaller than the value in AME2020 [25]. The mass-excess value of ^{72}As was improved by a factor of 38. It has an additional 0.08 keV/c^2 uncertainty in the reference mass, daughter ^{72}Ge.

Combining the new Q_{gs}^{EC} value together with the nuclear energy level data gives the final Q values for decays to the potential low Q-value states, see Table III. Also comparison to Q values obtained with AME2020 values is given. The results are also plotted in Fig. 6.

The AME2020 Q_{gs}^{EC} value, being 12.4 keV larger and having 4 keV uncertainty, could not unambiguously rule out these decays. Our results confirm that decays to any of the potential states are energetically forbidden. Decay to the 3327(3) keV 2^+ level is forbidden at the 1.8σ level, and others more than 42σ.

Though the EC/β^+ transitions studied here turned out to be energetically forbidden, this opens the door for the possibility to study another interesting decay type: radiative detour

TABLE III. Q values for the decay candidates to the excited states of the daughter nucleus ^{72}Ge obtained in this work compared to the values derived using AME2020 Q_{gs}^{EC} [25,26]. All data in the table are in keV. The first column gives the experimental excitation energy E^* [27] of the daughter state in ^{72}Ge. The second and third columns give the Q value using the Q_{gs} from AME2020 and from this work, respectively. The last column shows the confidence (σ) of the Q_{gs} being negative.

E^*	Q value (AME2020)	Q value (This work)	$Q/\delta Q$ (This work)
3325.01(3)	8.9(40)	−3.42(8)	43
3327(3)	6.9(50)	−5.4(30)	1.8
3338.0(3)	−4.1(40)	−16.41(31)	53
3341.76(4)	−7.9(40)	−20.17(8)	238
4358.7(3)	−2.8(40)	−15.11(31)	49

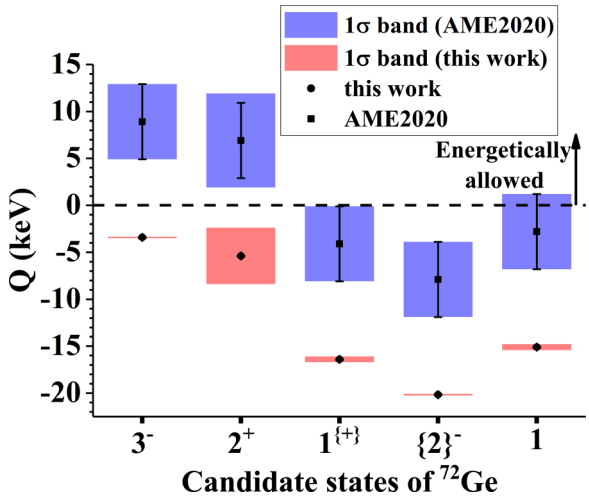

FIG. 6. Q values of the five potential candidate transitions of ^{72}As ground state β^+/EC decay to the potential excited states in the daughter ^{72}Ge from this work compared to the values derived using AME2020 Q_{gs}. The square and round points with 1σ error bars use ground-state to ground-state Q values from this work and AME2020, respectively, and show only the contribution from uncertainty of the ground-state to ground-state Q value. The total uncertainty (including both the Q_{gs} value and the excitation energy uncertainty) is indicated with shaded square areas.

transitions. In addition to regular EC/β^+ decay, a second-order process where a photon accompanies the lepton(s) is also possible. When the direct transition is hindered by angular momentum selection rules, a virtual transition via an excited state higher than the Q value can contribute significantly, as pointed out in Ref. [57]. Evidence of such a transition in ^{59}Ni was seen in Ref. [58], where a transition via a state 26 keV higher than the Q value was shown to contribute about 4% of the experimental γ spectrum. Since the probability of such a detour transition is proportional to $(E^* - E_\gamma)^{-2}$ [57], where E^* is the energy of the intermediate state and E_γ the energy of the emitted γ ray, a transition with a small negative Q value would be optimal for the experimental study of detour transitions. In the case of ^{72}As interesting transitions could proceed via the spin-1 state at 4358.7(3) keV. If this state turns out to have a negative parity, then the ground-state to ground-state transition could proceed via GT+E1 decay. However, finding transitions with even smaller negative Q values and less competing transitions would be even better. Such transitions are likely to be found when other possible ultralow Q-value transitions are investigated.

IV. CONCLUSION AND OUTLOOK

A direct high-precision ground-state to ground-state EC-decay Q-value measurement of ^{72}As $(2^-) \rightarrow$ ^{72}Ge (0^+) was performed using the PI-ICR technique at the JYFLTRAP Penning trap mass spectrometer. A Q value of 4343.596(75) keV was obtained and its uncertainty was improved by a factor of 54. A discrepancy of more than three standard deviations was found to the previously adopted value in the AME2020. Our updated and significantly more precise Q value is 12.4 keV smaller than the one adopted in AME2020. We confirmed that all five potential ultralow Q-value decay transitions, one through EC and four through β^+ decay are energetically forbidden at least at the 1.8σ level. This finding underlines the need to measure the Q values to high precision before attempts to detect such possible low Q-value decay branches is made, with the goal to realize these decays for neutrino mass determination. While the negative Q values exclude the use of ^{72}As to study neutrino mass, the small negative Q values could make it a candidate for the study of β-γ detour transitions proceeding via virtual states.

ACKNOWLEDGMENTS

We acknowledge the staff of the accelerator laboratory of University of Jyväskylä (JYFL-ACCLAB) for providing stable online beam and J. Jaatinen and R. Seppälä for preparing the production target. We thank the support by the Academy of Finland under the Finnish Centre of Excellence Programme 2012-2017 (Nuclear and Accelerator Based Physics Research at JYFL) and Projects No. 306980, No. 312544, No. 275389, No. 284516, No. 295207, No. 314733, No. 327629, and No. 320062. The support by the European Union's Horizon 2020 Research and Innovation Programme under Grant No. 771036 (ERC CoG MAIDEN) and under Grant Agreement No. 861198-LISA-H2020-MSCA-ITN-2019 is acknowledged.

[1] J. Suhonen and O. Civitarese, Phys. Rep. **300**, 123 (1998).
[2] F. T. Avignone, S. R. Elliott, and J. Engel, Rev. Mod. Phys. **80**, 481 (2008).
[3] H. Ejiri, J. Suhonen, and K. Zuber, Phys. Rep. **797**, 1 (2019).
[4] G. Drexlin, V. Hannen, S. Mertens, and C. Weinheimer, Adv. High Energy Phys. **2013**, 293986 (2013).
[5] M. Aker, K. Altenmüller, M. Arenz, M. Babutzka, J. Barrett, S. Bauer, M. Beck, A. Beglarian, J. Behrens, T. Bergmann, U. Besserer, K. Blaum, F. Block, S. Bobien, K. Bokeloh, J. Bonn, B. Bornschein, L. Bornschein, H. Bouquet, T. Brunst, T. S. Caldwell, L. La Cascio, S. Chilingaryan, W. Choi, T. J. Corona, K. Debowski, M. Deffert, M. Descher, P. J. Doe, O. Dragoun, G. Drexlin, J. A. Dunmore, S. Dyba, F. Edzards, L. Eisenblätter, K. Eitel, E. Ellinger, R. Engel, S. Enomoto, M. Erhard, D. Eversheim, M. Fedkevych, A. Felden, S. Fischer, B. Flatt, J. A. Formaggio, F. M. Fränkle, G. B. Franklin, H. Frankrone, F. Friedel, D. Fuchs, A. Fulst, D. Furse, K. Gauda, H. Gemmeke, W. Gil, F. Glück, S. Görhardt, S. Groh, S. Grohmann, R. Grössle, R. Gumbsheimer, M. Ha Minh, M. Hackenjos, V. Hannen, F. Harms, J. Hartmann, N. Haußmann, F. Heizmann, K. Helbing, S. Hickford, D. Hilk, B. Hillen, D. Hillesheimer, D. Hinz, T. Höhn, B. Holzapfel, S. Holzmann, T. Houdy, M. A. Howe, A. Huber, T. M. James, A. Jansen, A. Kaboth, C. Karl, O. Kazachenko, J. Kellerer, N. Kernert, L. Kippenbrock, M. Kleesiek, M. Klein, C. Köhler, L. Köllenberger, A. Kopmann, M. Korzeczek, A. Kosmider, A. Kovalík, B. Krasch, M. Kraus, H. Krause, L. Kuckert, B. Kuffner, N. Kunka, T. Lasserre, T. L. Le, O. Lebeda, M. Leber, B. Lehnert, J. Letnev, F. Leven,

S. Lichter, V. M. Lobashev, A. Lokhov, M. MacHatschek, E. Malcherek, K. Müller, M. Mark, A. Marsteller, E. L. Martin, C. Melzer, A. Menshikov, S. Mertens, L. I. Minter, S. Mirz, B. Monreal, P. I. Morales Guzmán, K. Müller, U. Naumann, W. Ndeke, H. Neumann, S. Niemes, M. Noe, N. S. Oblath, H. W. Ortjohann, A. Osipowicz, B. Ostrick, E. Otten, D. S. Parno, D. G. Phillips, P. Plischke, A. Pollithy, A. W. Poon, J. Pouryamout, M. Prall, F. Priester, M. Röllig, C. Röttele, P. C. Ranitzsch, O. Rest, R. Rinderspacher, R. G. Robertson, C. Rodenbeck, P. Rohr, C. Roll, S. Rupp, M. Ryšavý, R. Sack, A. Saenz, P. Schäfer, L. Schimpf, K. Schlösser, M. Schlösser, L. Schlüter, H. Schön, K. Schönung, M. Schrank, B. Schulz, J. Schwarz, H. Seitz-Moskaliuk, W. Seller, V. Sibille, D. Siegmann, A. Skasyrskaya, M. Slezák, A. Špalek, F. Spanier, M. Steidl, N. Steinbrink, M. Sturm, M. Suesser, M. Sun, D. Tcherniakhovski, H. H. Telle, T. Thümmler, L. A. Thorne, N. Titov, I. Tkachev, N. Trost, K. Urban, D. Vénos, K. Valerius, B. A. Vandevender, R. Vianden, A. P. Vizcaya Hernández, B. L. Wall, S. Wüstling, M. Weber, C. Weinheimer, C. Weiss, S. Welte, J. Wendel, K. J. Wierman, J. F. Wilkerson, J. Wolf, W. Xu, Y. R. Yen, M. Zacher, S. Zadorozhny, M. Zboeil, and G. Zeller, Phys. Rev. Lett. **123**, 221802 (2019).

[6] L. Gastaldo, K. Blaum, A. Doerr, C. E. Düllmann, K. Eberhardt, S. Eliseev, C. Enss, A. Faessler, A. Fleischmann, S. Kempf, M. Krivoruchenko, S. Lahiri, M. Maiti, Y. N. Novikov, P. C. Ranitzsch, F. Simkovic, Z. Szusc, and M. Wegner, J. Low Temp. Phys. **176**, 876 (2014), K. Blaum, A. Doerr, C. E. Duellmann, K. Eberhardt, S. Eliseev, C. Enss, A. Faessler, A. Fleischmann, L. Gastaldo, S. Kempf, M. Krivoruchenko, S. Lahiri, M. Maiti, Yu. N. Novikov, P. C.-O. Ranitzsch, F. Simkovic, Z. Szusc, and M. Wegner, arXiv:1306.2655.

[7] L. Gastaldo, K. Blaum, K. Chrysalidis, T. Day Goodacre, A. Domula, M. Door, H. Dorrer, C. E. Düllmann, K. Eberhardt, S. Eliseev, C. Enss, A. Faessler, P. Filianin, A. Fleischmann, D. Fonnesu, L. Gamer, R. Haas, C. Hassel, D. Hengstler, J. Jochum, K. Johnston, U. Kebschull, S. Kempf, T. Kieck, U. Köster, S. Lahiri, M. Maiti, F. Mantegazzini, B. Marsh, P. Neroutsos, Y. N. Novikov, P. C. Ranitzsch, S. Rothe, A. Rischka, A. Saenz, O. Sander, F. Schneider, S. Scholl, R. X. Schüssler, C. Schweiger, F. Simkovic, T. Stora, Z. Szücs, A. Türler, M. Veinhard, M. Weber, M. Wegner, K. Wendt, and K. Zuber, Eur. Phys. J.: Spec. Top. **226**, 1623 (2017).

[8] B. Alpert, M. Balata, D. Bennett, M. Biasotti, C. Boragno, C. Brofferio, V. Ceriale, D. Corsini, P. K. Day, M. De Gerone, R. Dressler, M. Faverzani, E. Ferri, J. Fowler, F. Gatti, A. Giachero, J. Hays-Wehle, S. Heinitz, G. Hilton, U. Köster, M. Lusignoli, M. Maino, J. Mates, S. Nisi, R. Nizzolo, A. Nucciotti, G. Pessina, G. Pizzigoni, A. Puiu, S. Ragazzi, C. Reintsema, M. R. Gomes, D. Schmidt, D. Schumann, M. Sisti, D. Swetz, F. Terranova, and J. Ullom, Eur. Phys. J. C **75**, 112 (2015).

[9] M. Faverzani, B. Alpert, D. Backer, D. Bennet, M. Biasotti, C. Brofferio, V. Ceriale, G. Ceruti, D. Corsini, P. K. Day, M. De Gerone, R. Dressler, E. Ferri, J. Fowler, E. Fumagalli, J. Gard, F. Gatti, A. Giachero, J. Hays-Wehle, S. Heinitz, G. Hilton, U. Köster, M. Lusignoli, M. Maino, J. Mates, S. Nisi, R. Nizzolo, A. Nucciotti, A. Orlando, L. Parodi, G. Pessina, G. Pizzigoni, A. Puiu, S. Ragazzi, C. Reintsema, M. Ribeiro-Gomez, D. Schmidt, D. Schuman, F. Siccardi, M. Sisti, D. Swetz, F. Terranova, J. Ullom, and L. Vale, J. Low Temp. Phys. **184**, 922 (2016).

[10] M. P. Croce, M. W. Rabin, V. Mocko, G. J. Kunde, E. R. Birnbaum, E. M. Bond, J. W. Engle, A. S. Hoover, F. M. Nortier, A. D. Pollington, W. A. Taylor, N. R. Weisse-Bernstein, L. E. Wolfsberg, J. P. Hays-Wehle, D. R. Schmidt, D. S. Swetz, J. N. Ullom, T. E. Barnhart, and R. J. Nickles, J. Low Temp. Phys. **184**, 958 (2016).

[11] E. G. Myers, A. Wagner, H. Kracke, and B. A. Wesson, Phys. Rev. Lett. **114**, 013003 (2015).

[12] E. Ferri, D. Bagliani, M. Biasotti, G. Ceruti, D. Corsini, M. Faverzani, F. Gatti, A. Giachero, C. Gotti, C. Kilbourne, A. Kling, M. Maino, P. Manfrinetti, A. Nucciotti, G. Pessina, G. Pizzigoni, M. Ribeiro Gomes, and M. Sisti, Phys. Procedia **61**, 227 (2015).

[13] M. Shamsuzzoha Basunia, Nucl. Data Sheets **143**, 1 (2017).

[14] D. A. Nesterenko, S. Eliseev, K. Blaum, M. Block, S. Chenmarev, A. Dörr, C. Droese, P. E. Filianin, M. Goncharov, E. Minaya Ramirez, Y. N. Novikov, L. Schweikhard, and V. V. Simon, Phys. Rev. C - Nuclear Physics **90**, 042501(R) (2014).

[15] A. Nucciotti, Nucl. Phys. B - Proc. Suppl. **229–232**, 155 (2012).

[16] S. Eliseev, K. Blaum, M. Block, S. Chenmarev, H. Dorrer, C. E. Düllmann, C. Enss, P. E. Filianin, L. Gastaldo, M. Goncharov, U. Köster, F. Lautenschläger, Y. N. Novikov, A. Rischka, R. X. Schüssler, L. Schweikhard, and A. Türler, Phys. Rev. Lett. **115**, 062501 (2015).

[17] P. C.-O. Ranitzsch, C. Hassel, M. Wegner, D. Hengstler, S. Kempf, A. Fleischmann, C. Enss, L. Gastaldo, A. Herlert, and K. Johnston, Phys. Rev. Lett. **119**, 122501 (2017).

[18] M. T. Mustonen and J. Suhonen, J. Phys. G: Nucl. Part. Phys. **37**, 64008 (2010).

[19] M. Mustonen and J. Suhonen, Phys. Lett. B **703**, 370 (2011).

[20] J. Suhonen, Phys. Scr. **89**, 54032 (2014).

[21] C. M. Cattadori, M. De Deo, M. Laubenstein, L. Pandola, and V. I. Tretyak, Nucl. Phys. A **748**, 333 (2005).

[22] B. J. Mount, M. Redshaw, and E. G. Myers, Phys. Rev. Lett. **103**, 122502 (2009).

[23] J. S. E. Wieslander, J. Suhonen, T. Eronen, M. Hult, V. V. Elomaa, A. Jokinen, G. Marissens, M. Misiaszek, M. T. Mustonen, S. Rahaman, C. Weber, and J. Äystö, Phys. Rev. Lett. **103**, 122501 (2009).

[24] V. A. Zheltonozhsky, A. M. Savrasov, N. V. Strilchuk, and V. I. Tretyak, Europhys. Lett. **121**, 12001 (2018).

[25] W. Huang, M. Wang, F. Kondev, G. Audi, and S. Naimi, Chin. Phys. C **45**, 030002 (2021).

[26] M. Wang, W. Huang, F. Kondev, G. Audi, and S. Naimi, Chin. Phys. C **45**, 030003 (2021).

[27] National Nuclear Data Center, available at https://www.nndc.bnl.gov, 2020.

[28] N. D. Gamage, R. Bhandari, M. Horana Gamage, R. Sandler, and M. Redshaw, Hyperfine Interact. **240** (2019).

[29] A. De Roubin, J. Kostensalo, T. Eronen, L. Canete, R. P. De Groote, A. Jokinen, A. Kankainen, D. A. Nesterenko, I. D. Moore, S. Rinta-Antila, J. Suhonen, and M. Vilén, Phys. Rev. Lett. **124**, 222503 (2020).

[30] R. Sandler, G. Bollen, N. D. Gamage, A. Hamaker, C. Izzo, D. Puentes, M. Redshaw, R. Ringle, and I. Yandow, Phys. Rev. C **100**, 014308 (2019).

[31] J. Karthein, D. Atanasov, K. Blaum, S. Eliseev, P. Filianin, D. Lunney, V. Manea, M. Mougeot, D. Neidherr, Y. Novikov, L. Schweikhard, A. Welker, F. Wienholtz, and K. Zuber, Hyperfine Interact. **240**, 1 (2019).

[32] J. Y. Mei, A. C. G. Mitchell, and C. M. Huddleston, Phys. Rev. **79**, 19 (1950).
[33] V. D. Vitman, B. S. Dzhelepov, and A. I. Medvedev, Izv. Akad. Nauk SSSR, Ser. Fiz. **32**, 1625 (1968).
[34] J. C. Hardy, L. C. Carraz, B. Jonson, and P. G. Hansen, Phys. Lett. B **71**, 307 (1977).
[35] S. Eliseev, D. Nesterenko, K. Blaum, M. Block, C. Droese, F. Herfurth, E. Minaya Ramirez, Y. N. Novikov, L. Schweikhard, and K. Zuber, Phys. Rev. C **83**, 038501 (2011).
[36] D. A. Nesterenko, L. Canete, T. Eronen, A. Jokinen, A. Kankainen, Y. N. Novikov, S. Rinta-Antila, A. de Roubin, and M. Vilen, Int. J. Mass Spectrom. **435**, 204 (2019).
[37] T. Eronen and J. C. Hardy, Eur. Phys. J. A **48**, 48 (2012).
[38] I. D. Moore, T. Eronen, D. Gorelov, J. Hakala, A. Jokinen, A. Kankainen, V. S. Kolhinen, J. Koponen, H. Penttilä, I. Pohjalainen, M. Reponen, J. Rissanen, A. Saastamoinen, S. Rinta-Antila, V. Sonnenschein, and J. Äystö, Nucl. Instr. Meth. Phys. Res. B **317**, 208 (2013).
[39] V. S. Kolhinen, T. Eronen, D. Gorelov, J. Hakala, A. Jokinen, K. Jokiranta, A. Kankainen, M. Koikkalainen, J. Koponen, H. Kulmala, M. Lantz, A. Mattera, I. D. Moore, H. Penttilä, T. Pikkarainen, I. Pohjlainen, M. Reponen, S. Rinta-Antila, J. Rissanen, C. Rodríguez Triguero, K. Rytkönen, A. Saastamoinen, A. Solders, V. Sonnenschein, and J. Äystö, Nucl. Instr. Meth. Phys. Res. B **317**, 506 (2013).
[40] J. Huikari, P. Dendooven, A. Jokinen, A. Nieminen, H. Penttilä, K. Peräjärvi, A. Popov, S. Rinta-Antila, and J. Äystö, Nucl. Instr. Meth. Phys. Res. B **222**, 632 (2004).
[41] P. Karvonen, I. D. Moore, T. Sonoda, T. Kessler, H. Penttilä, K. Peräjärvi, P. Ronkanen, and J. Äystö, Nucl. Instr. Meth. Phys. Res. B **266**, 4794 (2008).
[42] A. Nieminen, J. Huikari, A. Jokinen, J. Äystö, P. Campbell, and E. C. Cochrane, Nucl. Instr. Meth. Phys. Res. A **469**, 244 (2001).
[43] M. König, G. Bollen, H. J. Kluge, T. Otto, and J. Szerypo, Int. J. Mass Spectrom. Ion Processes **142**, 95 (1995).
[44] G. Gräff, H. Kalinowsky, and J. Traut, Z. Phys. A: At. Nucl. **297**, 35 (1980).
[45] D. A. Nesterenko, T. Eronen, A. Kankainen, L. Canete, A. Jokinen, I. D. Moore, H. Penttilä, S. Rinta-Antila, A. de Roubin, and M. Vilen, Eur. Phys. J. A **54**, 154 (2018).
[46] S. Eliseev, K. Blaum, M. Block, A. Dörr, C. Droese, T. Eronen, M. Goncharov, M. Höcker, J. Ketter, E. M. Ramirez, D. A. Nesterenko, Y. N. Novikov, and L. Schweikhard, Appl. Phys. B: Lasers Opt. **114**, 107 (2014).
[47] S. Eliseev, K. Blaum, M. Block, C. Droese, M. Goncharov, E. Minaya Ramirez, D. A. Nesterenko, Y. N. Novikov, and L. Schweikhard, Phys. Rev. Lett. **110**, 082501 (2013).
[48] G. Savard, S. Becker, G. Bollen, H. J. Kluge, R. B. Moore, T. Otto, L. Schweikhard, H. Stolzenberg, and U. Wiess, Phys. Lett. A **158**, 247 (1991).
[49] T. Eronen, V. V. Elomaa, U. Hager, J. Hakala, A. Jokinen, A. Kankainen, S. Rahaman, J. Rissanen, C. Weber, and J. Äystö, Acta Phys. Pol. B **39**, 445 (2008).
[50] Micro-channel plate detector with delay line anode, RoentDek Handels GmbH, Available at http://www.roentdek.de, 2020.
[51] M. Kretzschmar, in *Trapped Charged Particles and Fundamental Physics*, AIP Conf. Proc. No. 457 (AIP, New York, 1999), p. 242.
[52] A. Kramida, Yu. Ralchenko, J. Reader, and NIST ASD Team, NIST Atomic Spectra Database (ver. 5.8), National Institute of Standards and Technology, Gaithersburg, 2020, available: https://physics.nist.gov/asd, 2021.
[53] C. Roux, K. Blaum, M. Block, C. Droese, S. Eliseev, M. Goncharov, F. Herfurth, E. M. Ramirez, D. A. Nesterenko, Y. N. Novikov, and L. Schweikhard, Eur. Phys. J. D **67**, 146 (2013).
[54] A. Kellerbauer, K. Blaum, G. Bollen, F. Herfurth, H. J. Kluge, M. Kuckein, E. Sauvan, C. Scheidenberger, and L. Schweikhard, Eur. Phys. J. D **22**, 53 (2003).
[55] R. T. Birge, Phys. Rev. **40**, 207 (1932).
[56] E. A. Cornell, R. M. Weisskoff, K. R. Boyce, R. W. Flanagan, G. P. Lafyatis, and D. E. Pritchard, Phys. Rev. Lett. **63**, 1674 (1989).
[57] C. L. Longmire, Phys. Rev. **75**, 15 (1949).
[58] M. Pfützner, K. Pachucki, and J. Żylicz, Phys. Rev. C **92**, 044305 (2015).

Correction: A second affiliation has been added for the thirteenth author.

Second Correction: Support information in the Acknowledgment section was incomplete and has been fixed.